Anti-angiogenic and cytotoxic evaluation of green-synthesized Fe_2ZnO_4 nanoparticles against MCF-7 cell line

ASMA' AL-ZABIN[1], TUQA ABU THIAB[1], MALEK ZIHLIF[2], AFNAN AL-HUNAITI[3], HAMZEH J AL-AMEER[4], WAJDY AL-AWAIDA[5] and AMER IMRAISH[1]

[1]Department of Biological Sciences, School of Science, Biology Building; [2]Department of Pharmacology, Faculty of Medicine; [3]Department of Chemistry, School of Science, The University of Jordan, Amman 11942; [4]Department of Biotechnology, Faculty of Allied Medical Sciences, Al-Ahliyya Amman University, Amman 19328; [5]Department of Biology and Biotechnology, Faculty of Science, American University of Madaba, Madaba 17110, Jordan

Received September 21, 2023; Accepted November 27, 2023

DOI: 10.3892/br.2024.1724

Abstract. The use of plants for nanoparticle (NP) synthesis, grounded in green chemistry principles, is an environmentally friendly and economically viable approach. In the present study, the leaf extract of *Elaeagnus angustifolia L.* was used as a biosynthetic agent to generate bimetallic zinc oxide NPs. The present study investigated the effect of ZnO NPs on anti-angiogenesis and cell migration. Various bimetallic NPs, including zinc-iron oxide and nickel-zinc oxide, underwent characterization through Fourier-transform infrared spectroscopy and X-ray Diffraction within the 25-65˚ range. Confirmation of NP formation was determined by identifying the surface plasmon resonance peak. MTT assay was used to determine the cytotoxic properties of *E. angustifolia L.* extracts, ZnO NPs and associated metals in MCF-7 breast cancer cells. The plant extract demonstrated antiproliferative effects at 200 μg/ml, whereas *E. ang*-Fe_2ZnO_4 NPs showed varying cytotoxic effects based on concentration. The rat aortic ring and cell migration assays illuminated anti-angiogenic attributes, with the *E. ang*-Fe_2ZnO_4 NPs blocking blood vessel development entirely at 100 μg/ml, implying profound anti-angiogenic efficacy. Therefore, *E. ang*-Fe_2ZnO_4 NPs may serve a role in antiangiogenic therapy.

Introduction

Nanotechnology, a prominent domain in modern materials science, involves manipulation and comprehension of matter at atomic and molecular scales (1). Nanotechnology and nanoscience center around nanoparticles (NPs) 1-100 nm in diameter that exhibit unique physical, chemical and biological attributes (2). NPs have potential applications in medicine, electronics, chemistry, pharmaceuticals, agriculture and the food industry (3). Historically, the creation of NPs has necessitated costly and time-consuming physical and chemical processes demanding specialized equipment (4).

The chemical synthesis route for NPs has concerns over the incorporation of chemical compounds, use of toxic solvents and the emergence of noxious by-products (5). Consequently, a more eco-friendly, efficient and economical method termed 'green synthesis' has emerged, using natural biological entities such as plants, fungi and bacteria for NP creation (6). Empirical studies underscore plants as the optimal choice for large-scale biosynthesis (6,7). Green synthesis of metal NPs, predominantly with plants as the reductive agents, has gained traction (6).This methodology coats NPs, enhancing their biological effect. Furthermore, plant-derived NPs demonstrated enhanced stability and diversified morphological features compared with conventional synthesis (8).

Metal NPs with distinct physical and chemical properties have garnered scientific attention (2). Owing to high surface-to-volume ratio, they serve as potential drug carriers, and can cross the blood-brain barrier and epithelial cell junctions to access remote targets (9). Their antiangiogenic capabilities have been demonstrated in numerous *in vitro* models, including chick embryo chorioallantoic membrane (CAM), aortic ring and Matrigel-endothelial culture assay (4,6).

Angiogenesis, the formation of new blood vessels from pre-existing ones, plays a pivotal role in tissue development, wound healing and the prognostic evaluation of cancer (10). Various angiogenic promoters and suppressors regulate this process (11). The equilibrium between pro-angiogenic molecules, such as vascular endothelial growth factor (VEGF) and fibroblast growth factor-2 (12), and their antagonists, such as angiostatin and angiopoietin 2, is crucial. Disruptions in this balance instigate pathological conditions (13). Numerous studies have aimed to modulate angiogenesis as its excess can cause cancer, arthritis, asthma, psoriasis and diabetic blindness (13,14). Given the role of angiogenesis in tumor evolution and metastasis, therapeutic interventions targeting its

Correspondence to: Dr Amer Imraish, Department of Biological Sciences, School of Science, Biology Building, The University of Jordan, Queen Rania Al-Abdullah Street, Amman 11942, Jordan
E-mail: a.imraish@ju.edu.jo

Key words: nanoparticle, anti-angiogenic, cytotoxic, *Elaeagnus angustifolia L.* extract, MCF-7, VEGF, ELISA

inhibition have been identified such as strategies blocking the VEGF pathway, pivotal for cancer cell dynamics (15). Metal oxide and carbon-based nanomaterials with reduced toxicity have shown potential in suppressing angiogenic pathways, making them suitable candidates for therapeutic applications in cancer and other disorders (16).

Historically, medicinal plants have been repositories of bioactive compounds. At present, 40% of prescription drugs owe their origins to herbs (17-19). The medicinal plant *Elaeagnus angustifolia (E. ang)*, a member of the Elaeagnaceae family commonly termed oleaster or Russian olive, has numerous therapeutic applications (20). For example, the leaf extract of *E. ang* has efficacy in managing chronic bronchitis (21), expediting wound healing (22) and serving as a muscle relaxant (23). Its fruit extract ameliorates pain in rheumatoid arthritis, asthma, nausea and vomiting and aids wound healing in skin tissues (24,25). Pharmacological studies have shown that *E. ang* L. has anti-inflammatory, antimicrobial, antinociceptive and anti-oxidant effects that might be used for treating a number of distresses (26,27). *E. ang* is commonly found naturally in Jordan (28).

Synthesis of zinc oxide NPs using *E. ang* combines the therapeutic potentials of both entities, especially in wound healing and cellular migration (16). The fusion of zinc mineral and plant extract might potentiate synergistic effects on angiogenesis and wound healing. The present study aimed to elucidate the influence of green composite bimetallic NPs on angiogenesis through *in vitro* aortic assay and wound healing experiments.

Materials and methods

Plant collection. E. ang L. was collected during its blossoming phase in April, 2021, from a cultivated region on Istiqlal Street, Amman, Jordan. The identification of the plant was verified by Professor Barakat Abu Irmaileh (Faculty of Agriculture, The University of Jordan, Amman, Jordan). A voucher specimen (no. ELEA-1FMJ) was deposited in the Department of Pharmaceutical Sciences, School of Pharmacy, The University of Jordan. Following collection, the leaves were passively air-dried in the shade for ~1 week until a consistent weight was observed. Once dried, the leaves were ground to achieve a fine consistency. This powdered form was then utilized to prepare the aqueous extract.

Preparation of the aqueous leaf extract of E. ang L. Leaves of *E. ang L.* were carefully rinsed with deionized water, then dried at 30˚C in a contamination-free setting. A total of ~200 g dried leaves were finely ground into a powdery consistency using a pestle and mortar. This powdered material was combined with 500 ml deionized water. The mixture was subjected to reflux for 4 h in an oil bath at 90˚C. After the reflux period, the solution was allowed to return to room temperature and filtered through Whatman No.1 filter paper to remove any solid residues. The resulting extract of *E. ang L.* was used as a reducing agent in NP synthesis.

Synthesis and characterization of bimetallic ZnO_4 NPs (Fe_2ZnO_4). The aqueous extract was mixed with an equivalent volume of 1 mM iron (III) chloride hexahydrate ($FeCl_3 \cdot 6H_2O$) and 1 mM zinc acetate [$Zn(OAc)_2$]. This mixture was stirred for ~1 h and was then exposed to ultrasonic waves in an ultrasonic bath for 30 min at room temperature. pH of the reaction mixture was maintained at 10-12 using a NaOH solution. NPs were separated by centrifugation at 7,500 x g for 10-15 min at room temperature, and dried in an oven at 80˚C for 4 h. NPs were washed multiple times with water until a neutral pH was achieved, as previously described (24).

Synthesis of bimetallic Fe_2ZnO_4 NPs. Metal salt solutions (1 mM) (silver nitrate and zinc acetate) were combined and heated to 80˚C for ~30 min. Following this, 50 ml *E. ang L.* extract was gradually added using a burette until the total volume reached 90 ml. This blend was stirred continuously at 80˚C for 1 h. After stirring, the solution was allowed to settle, leading to the formation of a precipitate. This precipitate underwent sonication in an ultrasonic chamber for 30 min, as previously described (25). The pH was then adjusted to 10-12 using a NaOH solution. The NPs were isolated by centrifugation at 7,500 x g for 10-15 min at room temperature. NPs were dried in an oven set at 80˚C for 4 h and the remaining solid was washed several times with water until a neutral pH was reached, as previously described (29).

Characterization of bimetallic NPs. The composition of the particles was confirmed via Fourier-transform infrared spectroscopy (FTIR) analysis. The crystallinity of the bimetallic NPs was investigated using x-ray diffraction (XRD) analysis, covering a range of 25-65˚.

Crystallographic structure of the prepared NPs was determined by powder X-ray diffraction pattern. The infrared (IR) spectrum was acquired using a Perkin Elmer RX-FTIR spectrometer with potassium bromide disc and scanning range of 4,000-300 cm^{-1}.

Cell culture. Cell lines were sourced from the American Type Culture Collection (ATCC), including the breast cancer cell line MCF-7 (cat. no. ATCC® HTB-22TM) and a standard dermal fibroblast cell line (BJ; cat. no. ATCC® CRL-2522). The cell lines were cultured in RPMI-1640 medium (HyClone; Cytiva) in vented 75 cm^2 culture flasks. The medium was supplemented with 10% (v/v) heat-inactivated fetal bovine serum (Gibco, Thermo Fisher Scientific) antibiotics (100 U/ml penicillin and 100 g/ml streptomycin), 2 mM L-glutamine and 25 μM HEPES. These flasks were kept in an atmosphere of 5% CO_2 and 95% air and a set temperature of 37˚C. All cell experiments were performed in a class II biological safety cabinet to ensure sterility. MCF-7 breast cancer and the standard fibroblast cells were seeded in 96-well plates at densities of 7,000 and 9,000 cells/well, respectively, and were then incubated at 37˚C overnight adhere to the plate well surface.

In vitro anti-proliferative and cytotoxicity assay. The cytotoxicity of bimetallic NPs on MCF-7 and fibroblast cells was evaluated by MTT assay, as previously described (30). A total of 7,000 MCF-7 cells were seeded in duplicate in each well of a 96-well plate and incubated for 24 h at 37˚C. A total of 10 mg/ml bimetallic *E. ang*-Fe_2ZnO_4 and Fe_2ZnO_4 NPs and 10 mM aqueous leaf extract of *E. ang L.* was dissolved in 1%

dimethyl sulfoxide (DMSO). Seven distinct concentrations, ranging from 200, 100, 50, 25, 12.5, 6.25 and 3.125 μg/ml, were tested. After 72 h incubation at 37˚C, the viability of the cells was assessed. Doxorubicin was used as a positive control. Spectrophotometric measurements were employed to ascertain the antiproliferative activity across varied concentrations of *E. ang*-Fe_2ZnO_4. The absorbance of these solutions was determined at 570 nm. Dose-response curves were analyzed by regression analysis using sigmoidal curves [log(concentration) vs. normalized absorbance]. The half-maximal inhibitory concentration (IC_{50}) was determined with GraphPad Prism software version 8.0.0 (La Jolla, CA).

Ex vivo aortic ring assay. Rat aortic ring assay was conducted using eight adult (8-10 weeks) male Wister albino rats (*Rattus norvegicus*; weight, 200-250 g; Animal House Unit, The University of Jordan). Rats were housed in The University of Jordan Animal House Unit at 22±1˚C under a 12/12-h light/dark cycle, and the humidity range was 50-60% with free access to food and water. Experimental procedures were approved by the scientific research committee (The Institutional Review Board of the University of Jordan) at the University of Jordan (approval no. 47-2022). All experiments were performed according to the Animal (Scientific Procedure) Act 1986 and International Association for the Study of Pain guidelines (13). Rats were euthanized using CO_2 overdose followed by decapitation. A fill rate of 30-70% of the chamber volume/min with CO_2 was used to induce rapid unconsciousness with minimal distress to the animals.

Immediately post-extraction, the aortae were submerged in a cold sterile 1% PBS solution in a Petri dish. Using a dissecting microscope for precision, extraneous connective tissue was removed. The aortae, after cleaning with PBS, were sectioned into ~1 mm thick rings using a surgical scalpel. These segments were immersed in cold PBS solution and stored on ice until use.

Each aortic ring was positioned within a 48-well plate using cold pipette tips. Rings were immersed in 25 μl low growth factor Matrigel™ (Corning, Inc.) and were placed in pairs. Following 30 min incubation at 37˚C to allow coagulation, aliquots of 250 μl, with concentrations 100, 50, 25, 12.5, 6.25 and 3.125 μg/ml, of the three different extracts diluted in RPMI-1640 were added. For the control group, DMSO was used at a concentration of 100 μg/ml. The plate was then incubated at 37˚C. On day 4, medium was refreshed. On day 5, images were captured using an inverted light microscope at 4x magnification.

The angiogenic response was quantified by measuring the extension of blood vessels from the primary ring explants using ImageJ software1.29 (National Institutes of Health). For each ring, ≥35 comparable structures, evenly spaced around the ring, were measured (26).

Data were analyzed with GraphPad Prism 8 software. The elongation distance of the emerging vessels for each ring was recorded as the mean of percentage inhibition relative to the unaltered control (n=2) (27). Vessel lengths were expressed in arbitrary units and the inhibition of vessel formation was as follows: Angiogenic inhibition=[1-(A0/A)] x100, where A0 represents vessel growth distance in treated rings and A signifies the vessel growth distance in control rings.

Treatment of MCF-7 with E. ang-Fe_2ZnO_4 and Fe_2ZnO_4 NPs and organic extract. A total of ~1x10^5 MCF-7 cells were seeded in a 24-well plate and incubated overnight at 37˚C in 5% CO_2 to ensure adhesion. A 10 mg/ml stock solution of *E. ang*-Fe_2ZnO_4 and Fe_2ZnO_4 NPs and organic extract was then prepared using DMSO. Serial dilutions were made in RPMI-1640 (HyClone; Cytiva) complete media at 200.00, 100.00, 50.00, 25.00, 12.50 and 6.25 μg/ml *E. ang*-Fe_2ZnO_4 NPs and organic extract. For Fe_2ZnO_4 NPs, dilutions were made to 200, 100, 50 and 25 μg/ml based on cytotoxicity and anti-angiogenic effects. DMSO concentration was <1% for all treatments. Quadruplicate samples were used for every concentration. Control wells, containing only the complete medium, were also included in each assay. Following 72 h incubation at 37˚C with the treatments, conditioned media was harvested and stored at -80˚C until use.

Measurement of VEGF concentration using ELISA. Secretion levels of VEGF in conditioned media from both treated and control (untreated) cells were quantified by ELISA, as previously described (31). Human VEGF (cat. no. #DY293B05; R&D Systems, Inc.) ELISA kit was used to measure the concentration of VEGF secreted in conditioned media, following the manufacturer's protocol. Concentrations were calculated using Microsoft Excel software (Microsoft Office professional plus 2016) using the standard curve equation and further analyzed using Prism 8 statistical analysis software (GraphPad Software, Inc.).

Statistical analysis. Statistical analysis was performed using GraphPad Prism software, version 8.0.0. IC50 values for each tested NP were derived by fitting the observed data to a logarithmic trend line depicted on the cytotoxicity graphs (log concentration against inhibition percentage). Data are presented as the mean ± SEM. Each experiment was performed in triplicate. To assess number and length of blood vessels, images were analyzed using the ImageJ 1.29 (National Institutes of Health). Data were analyzed using one-way ANOVA followed by Bonferroni's multiple comparisons post hoc test. $P<0.05$ was considered to indicate a statistically significant difference.

Results

To characterize synthesized NPs, XRD, FTIR spectroscopy and ζ potential measurements were performed. Formation of the bimetallic ZnO NPs was confirmed by the XRD patterns (Fig. 1). Distinct peaks consistent with the standard data for the spinel (Franklinite) phase (ICSD card no. 30,860) were demonstrated (8). Furthermore, the characterization data obtained for spinel Fe_2ZnO_4 were consistent with previously documented XRD pattern for NPs (29), exhibiting mean particle size of 18 nm (Fig. 1).

Structure of *E. ang*-Fe_2ZnO_4 was determined by the X-ray diffraction pattern. Fe_2ZnO_4 NPs had mean particle size of 90.22 nm. A lattice constant value of 299.96 and a corresponding d-spacing value of 90.22 nm were also identified,

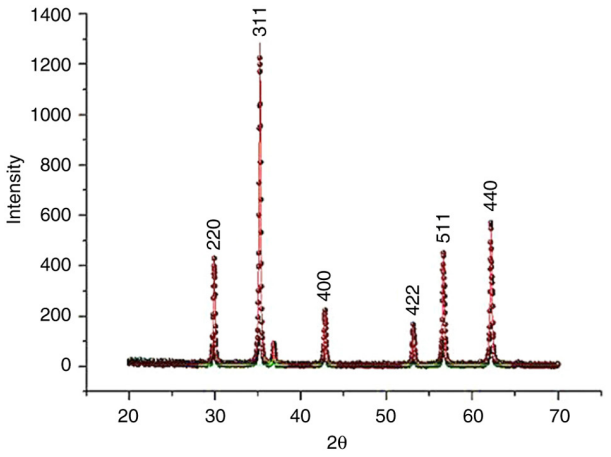

Figure 1. X-Ray Diffraction patterns of bimetallic iron zinc oxide (Fe_2ZnO_4) nanoparticles that have been coated with an aqueous extract of *Elaeagnus angustifolia L*.

indicating the crystalline disposition and intrinsic interplanar spacing of Fe_2ZnO_4 NPs (Fig. 1).

To elucidate potential interactions between bimetallic ZnO NPs and bioactive constituents of E. ang L. aqueous leaf extract, FTIR spectrum of the bimetallic NPs was analyzed and it shows the confrmed the vibrational stretching modes of metal-oxygen bonds in ZnFe2O4 nanoparticles. (Fig. 2). Additionally, the charging characteristic of the prepared NPs were inspected by zeta potential with -21 mV which indicate that the prepared nanoparticles are likely to exhibit good stability and resist agglomeration. (Fig. 2).

Anti-proliferative effect and cytotoxicity of bimetallic E. ang-Fe_2ZnO_4 and ZnO NPs. IC_{50} of *E. ang*-Fe_2ZnO_4 and metallic ZnO NPs and *E. ang L*. aqueous leaf extract was evaluated in MCF-7 and fibroblast cell lines using MTT assay. Cytotoxicity of *E. ang*-Fe_2ZnO_4 NPs and Fe_2ZnO_4 NPs in MCF-7 cells were assessed in comparison with the fibroblast cell line. Further, the cytotoxicity exhibited by *E. ang*-Fe_2ZnO_4 was determined in both MCF-7 and fibroblast cell lines using IC_{50}. Fe_2ZnO_4 NPs had IC_{50} values of 3.574 μg/ml for MCF-7 cells and 61.290 μg/ml for fibroblasts (Figs. S1 and S2). Conversely, *E. ang*-Fe_2ZnO_4 NPs demonstrated an augmented resilience, producing an IC_{50} value >200 for MCF-7 and 67.15 μg/ml for fibroblasts. The isolated *E. ang L*. aqueous extract had IC_{50} values >200 for MCF-7 and 78.65 μg/ml for fibroblasts. Doxorubicin, a chemotherapeutic agent, had IC_{50} values of 0.350±0.025 for MCF-7 and 7.037±2.960 μM for fibroblasts, underscoring its cytotoxic effect.

Anti-angiogenic activity. The angiogenic potential of *E. ang*-Fe_2ZnO_4 and Fe_2ZnO_4 NPs and the aqueous extract of *E. ang* L. leaf was evaluated utilizing the rat aortic ring assay. Angiogenesis was quantified by measuring the extension of vessels emanating from the primary ring (Fig. S3). A significant inhibition of micro-vessel outgrowth from the aortic rings was observed when treated with *E. ang*-Fe_2ZnO_4 NPs in a dose-dependent manner (Fig. 3). At a concentration of 100 μg/ml, the mean inhibition of 98.71±0.36% was noted compared with the control group. At 50.0, 25.0 and 12.5 μg/ml, the growth of new blood vessels was significantly decreased by 98.190±0.365, 96.650±10.365 and 81.680±1.090%, respectively. Moreover, the concentration 6.25 μg/ml significantly decreased the growth of new blood vessels by 47%±1.075. However, 3.125 μg/ml did not significantly inhibit micro-vessel outgrowth (5.30±0.36%).

Significant inhibition of micro-vessel outgrowth from the aortic rings was observed when treated with Fe_2ZnO_4 NPs in a dose-dependent manner (Fig. 4). At 100 μg/ml, a significant inhibition of 86.32±1.09% was noted in comparison with the control group. Moreover, concentrations of 50.0, 25.0 and 12.5 μg/ml attenuated the growth of new blood vessels by 81.300±3.102, 67.740±1.094 and 48.640±1.095%, respectively. A concentration of 3.125 μg/ml did not significantly inhibit micro-vessel outgrowth (3.741±1.095%).

Micro-vessel outgrowth from the aortic rings was observed to be significantly inhibited following exposure to *E. ang* L. extract at 100 μg/ml (96.38±0.73% compared with the control; Fig. 5). *E. ang* L. aqueous extract also significantly decreased micro-vessel outgrowth by ~94.580±1.090, 85.030±1.450 and 50.710±1.094 at concentrations of 50.0, 25.0 and 12.5 μg/ml, respectively. At 3.125 μg/ml, *E. ang* L. extract resulted in growth inhibition of 1.680±1.095%.

VEGF secretion by MCF-7 cells. The secretion of VEGF was significantly inhibited by 200 μg/ml *E. ang*-Fe_2ZnO_4 NP, reducing to ~0.427 times that of the control. Also, significant 0.690 and 0.814 times suppression of VEGF protein was observed upon treatment with 50 and 25 μg/ml, respectively; other concentrations showed insignificant reduction of protein levels of VEGF (Fig. 6).

At a concentration of 200 μg/ml, VEGF secretion in response to Fe_2ZnO_4 -NPs decreased to ~0.348 times that observed in the control group, but this reduction was not statistically significant. The other concentrations also did not cause any significant change in VEGF secretion (Fig. 7).

VEGF secretion, upon exposure to 200 μg/ml organic extract, was observed to be significantly decreased by 0.366 times relative to the levels in the control. However, no other concentrations caused a significant decline in VEGF protein levels (Fig. 8).

Discussion

Research is focused on green synthesis of metallic NPs, a low-cost, environmentally friendly method that uses natural organisms as a reduction source to produce safer, more biologically functional NPs (32). Here, Fe_2ZnO_4 bimetallic NPs were phytosynthesized using an aqueous extract of *E. ang*. It is hypothesized that these bimetallic nanoparticles have anti-inflammatory and antioxidant properties.

X-ray patterns displayed sharp peaks, aligning with the standard data for all *E. ang*-Fe_2ZnO_4 (29). The mean of crystallite size was between 5.10 and 114.41 nm (29). Particle size serves a key role in cellular transport. Smaller particles more readily penetrate the plasma membrane, making NPs with diameter <100 nm suitable for various drug delivery systems. Studies indicate that due to their small size, ZnO NPs can traverse blood capillaries and interact with multiple cells in different tissues (21,22).

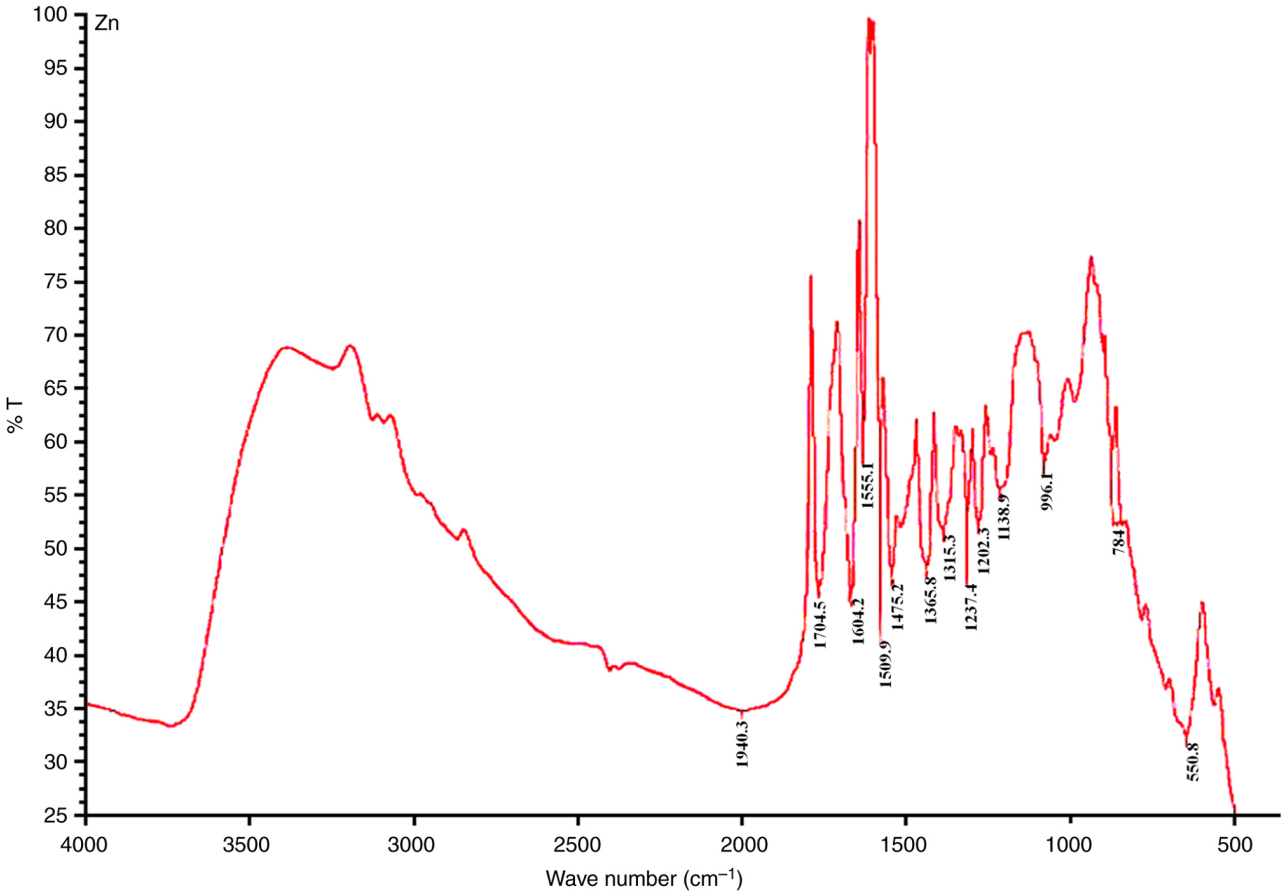

Figure 2. Fourier-Transform Infrared (FTIR) spectrum of coated bimetallic iron zinc oxide (Fe_2ZnO_4) nanoparticles with *Elaeagnus angustifolia* L. aqueous extract. T, Transmission.

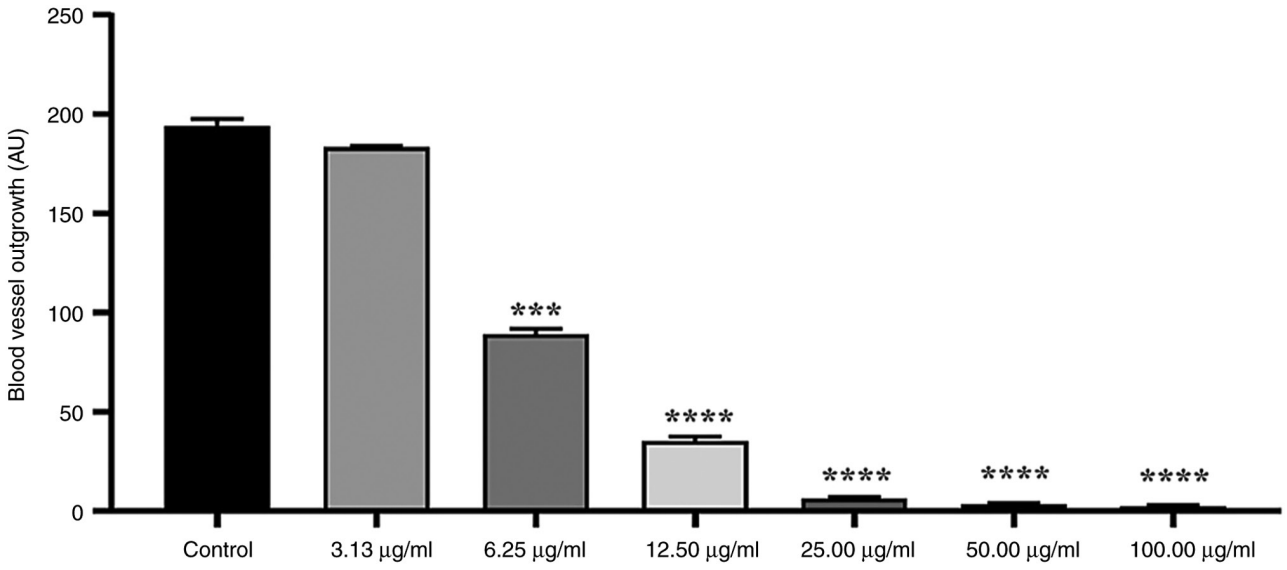

Figure 3. Dose response of *Elaeagnus angustifolia* L.-Fe_2ZnO_4 nanoparticles in rat aortic ring assay. The angiogenic response was determined by measuring the length of blood vessel outgrowth from the primary tissue explants. ***P<0.001, ****P<0.0001 vs. control.

The present results align with prior research, demonstrating that green synthesis of bimetallic ZnO NPs via plant extracts produces stable, nano-sized ZnO NPs (8). The present study investigated the anti-angiogenesis and cytotoxic effects of *E. ang*-Fe_2ZnO_4 and zinc-iron oxide, nickel-zinc oxide, copper-zinc oxide, and manganese-zinc oxide NPs. The cytotoxicity of these NPs and *E. ang L.* extract on MCF-7 and fibroblast cells was assessed. Bimetallic NPs exhibited notable cytotoxic effects, while *E. ang*-Fe_2ZnO_4 NPs and *E. ang L.* leaf extract did not demonstrate toxicity

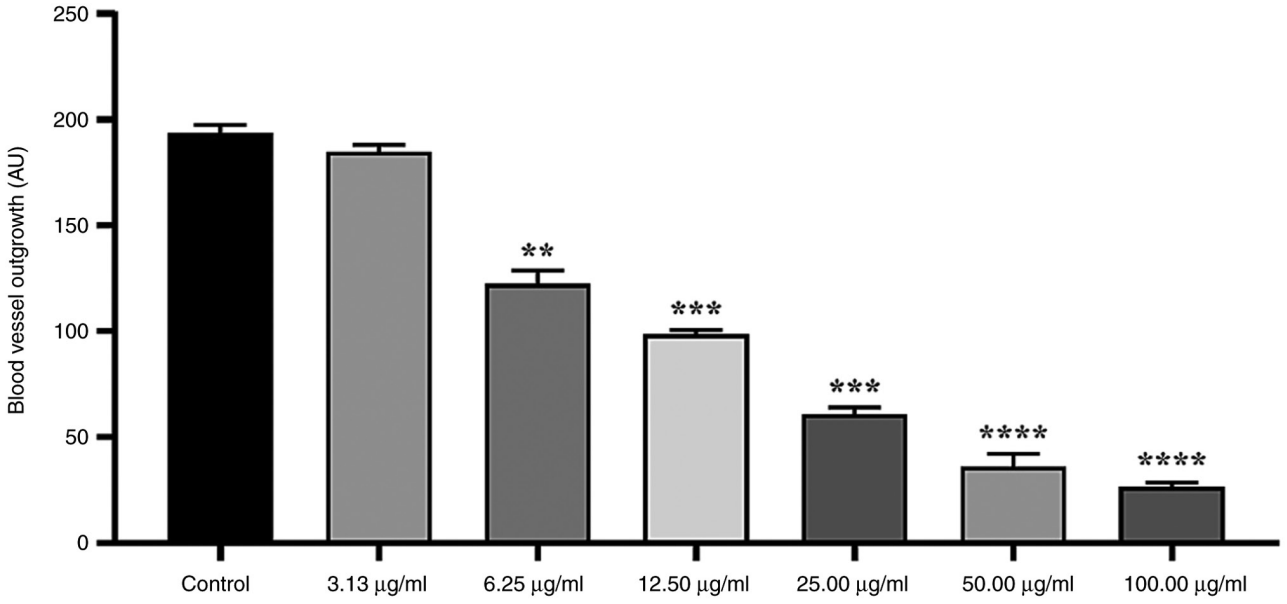

Figure 4. Dose response of bimetallic Fe_2ZnO_4 nanoparticles in the rat aortic ring assay. The angiogenic response was determined by measuring the length of blood vessel outgrowth from the primary tissue explants. **P<0.01, ***P<0.001, ****P<0.0001 vs. control.

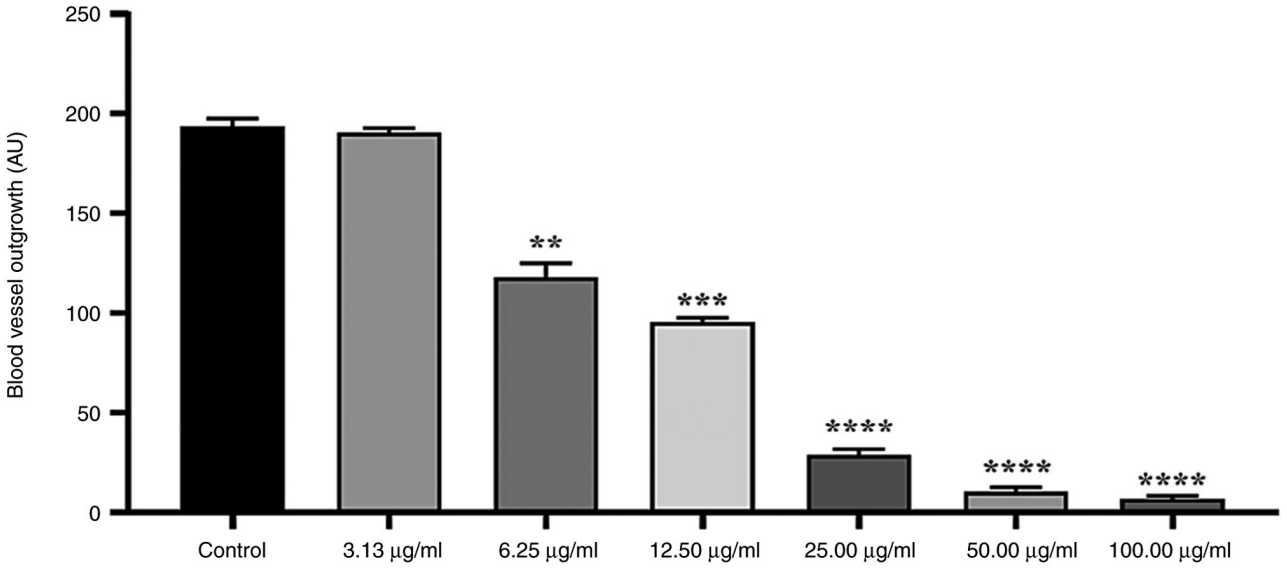

Figure 5. Dose response of *Elaeagnus angustifolia* L. extract in the rat aortic ring assay. The angiogenic response was determined by measuring the length of blood vessels outgrowth from the primary tissue explants. The angiogenic response was determined by measuring the length of blood vessel outgrowth from the primary tissue explants. **P<0.01, ***P<0.001, ****P<0.0001 vs. control.

against MCF-7 cells at the highest concentration (200 μg/ml). Prior study found low cytotoxicity of Fe_2ZnO_4 coated with *Boswellia carteri* resin against Raw 264.7 macrophage cells (29). A previous study also highlighted the anticancer potential of green-synthesized silver NPs derived from *Fagonia indica* extract against MCF-7 cells (33). Similarly, at concentrations >175 μg/ml, green-synthesized ZnO NPs decrease human hepatocyte (HepG2) cell viability to <40%; at the maximum concentration (2,800 μg/ml), >95% of the cells die, in addition to anti-angiogenic effects demonstrated by CAM assay (32).

The present findings suggest that green NP synthesis, may provide a protective effect against cell toxicity by masking metallic NPs, which results in lower cytotoxic effect on cells (34).

Angiogenesis, a key physiological process responsible for novel blood vessel formation, is vital in embryonic development, ovulation (10) and wound healing (3).Two primary methods for modulating angiogenesis exist: Direct and indirect pathways. The direct pathway involves modulating the ability of vascular endothelial cells to proliferate, migrate and respond to angiogenic factors such as VEGF. The indirect pathway is based on the capacity to affect the expression and activity of angiogenic factors that induce angiogenesis. This includes controlling expression of receptors on endothelial cells such as tyrosine kinase receptor IGF-IR and chemokine receptor CCR7 (3).

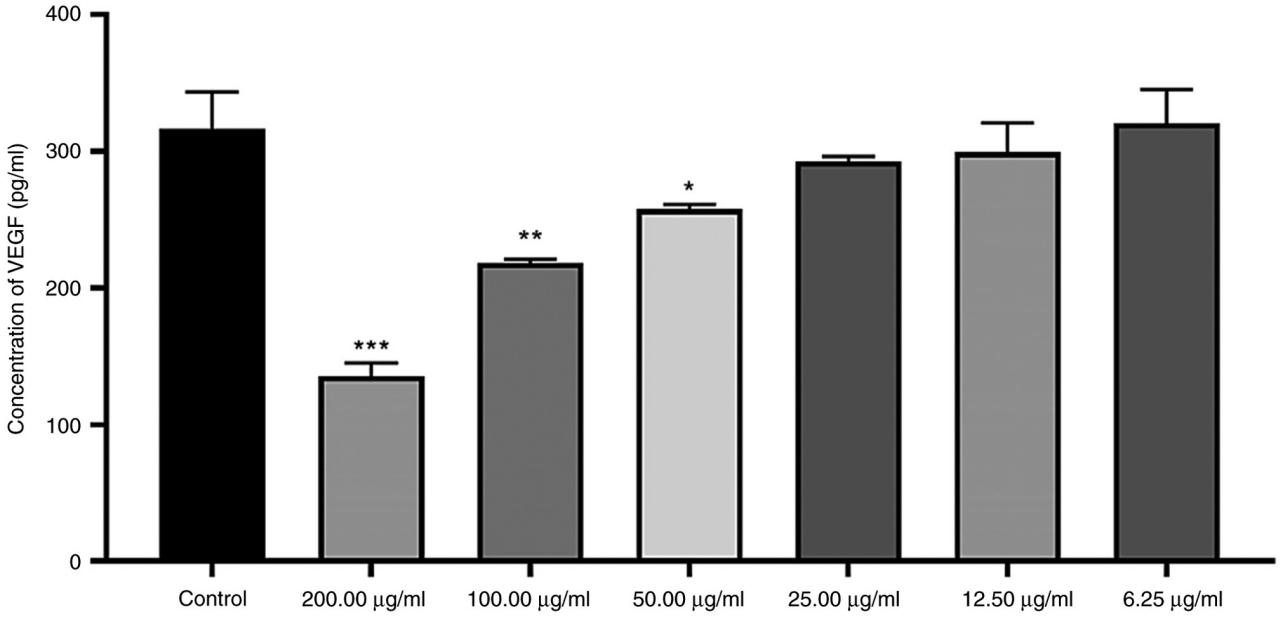

Figure 6. Levels of secreted VEGF from breast cancer MCF-7 cells treated with *Elaeagnus angustifolia* L.-Fe_2ZnO_4 nanoparticles. *P<0.05, **P<0.01, ***P<0.001 vs. control.

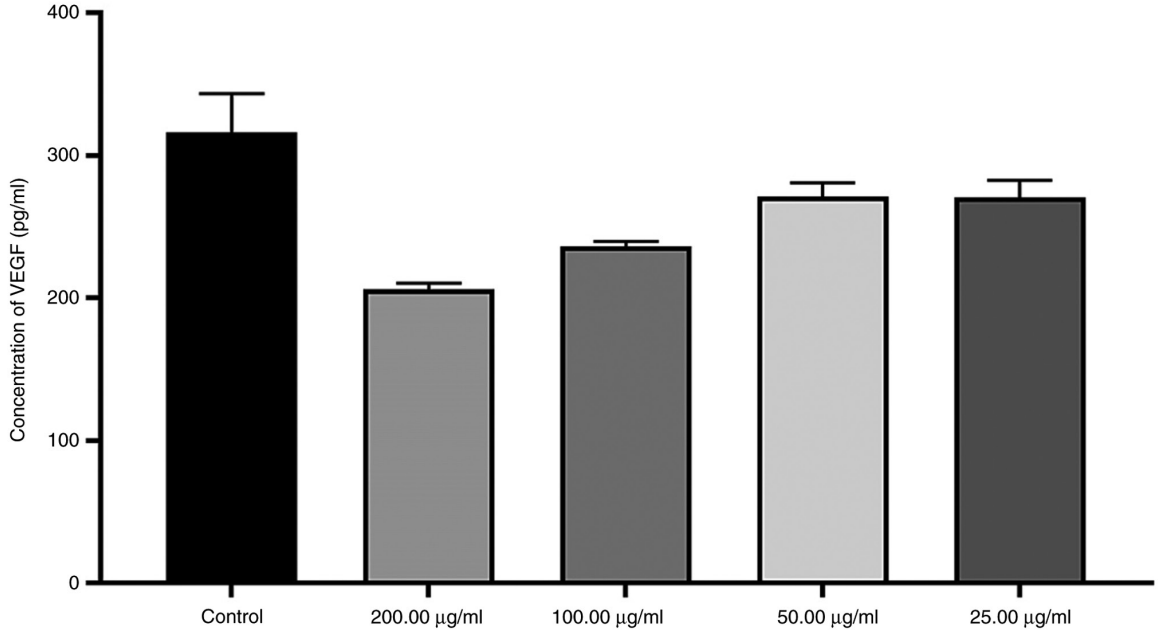

Figure 7. Levels of secreted VEGF from breast cancer MCF-7 cells treated with bimetallic Fe_2ZnO_4 nanoparticles.

The present study investigated anti-angiogenic potential via rat aortic ring assay. Bimetallic Fe_2ZnO_4 and *E. ang*-Fe_2ZnO_4 NPs and *E. ang* L. extract exhibited high inhibitory activity at 100 μg/ml, resulting in >85% mean inhibition. *E. ang*-Fe_2ZnO_4 NPs continued to show a significant inhibitory activity at 6.25 μg/ml with 39.10±3.65% vessel outgrowth inhibition. By comparison with Fe_2ZnO_4 NPs and the extract of *E. ang* L., *E. ang*-Fe_2ZnO_4 NPs significantly inhibited growth of vessels, indicating an additive effect for green synthesis of Fe_2ZnO_4 NPs.

Anti-angiogenic properties of green-synthesized ZnO NPs generated using extract of *Hyssops officinalis L.* have been investigated via CAM assay and show considerable decrease in the number and length of blood vessels and suppression of vessel formation by inducing death in endothelial cells (4). *In vivo* and *in vitro* assays have been used to identify angiogenic activators and inhibitors (10,14). Typically, CAM and aortic ring *in vivo* assays are used to investigate angiogenic activity. Rat aorta rings offer a sensitive assay for the investigation of angiogenic activators and inhibitors. *E. ang*-Fe_2ZnO_4 NPs had a significant inhibitory activity on VEGF expression in MCF-7 cells. Bimetallic Fe_2ZnO_4-NPs and *E. ang* L. extract showed inhibitory effects at 200 μg/ml, while lower concentrations elevated the secretion of VEGF compared with

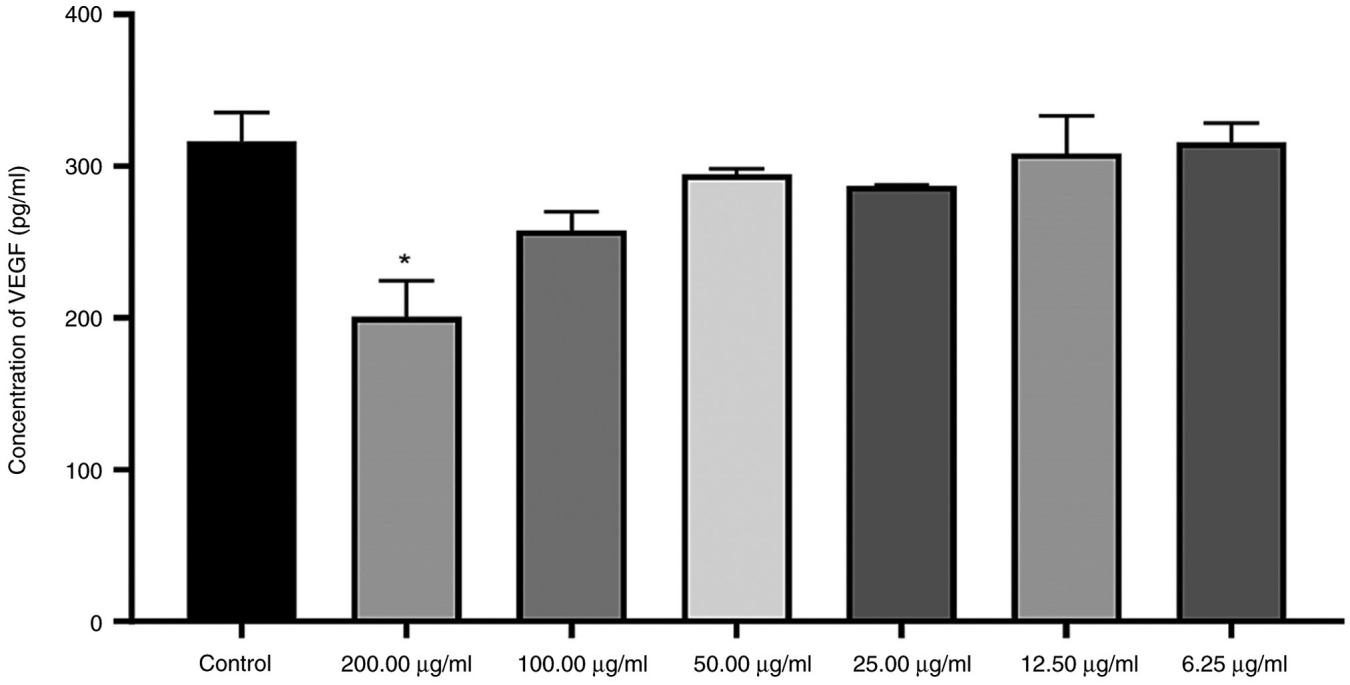

Figure 8. Levels of secreted VEGF from breast cancer MCF-7 cells treated *Elaeagnus angustifolia* L. aqueous extract. *P<0.05 vs. control.

E. ang-Fe_2ZnO_4 NPs. It was hypothesized that *E. ang*-Fe_2ZnO_4 had an additive impact in reducing VEGF secretion. These data are consistent with a previous study that demonstrated that ZnO NPs suppress the expression of genes encoding VEGF and VEGF receptor (35).

Nevertheless, the present study has limitations that must be addressed. The present study only investigated a limited number of these angiogenesis biomarkers; the effect of *E. ang* water extract on different angiogenesis biomarkers should be assessed in the future, including the cell cycle regulators.

The present current investigation used leaf extract of *E. ang* L. for the green synthesis of bimetallic zinc oxide NPs, which is a method that is both environmentally friendly and cost-effective. The synthesized NPs, particularly *E. ang*-Fe_2ZnO_4 NPs, exhibited potent anti-angiogenic and cytotoxic effects against MCF-7 breast cancer cells, while maintaining minimal toxicity toward healthy cells. These findings suggest NPs are promising candidates for anti-cancer therapy, especially in targeting angiogenesis. Bimetallic NPs require *in vivo* validation to ensure their efficacy and safety for potential clinical applications. Furthermore, standardization of *E. ang* aqueous extract should be performed to obtain uniform products for experimental testing, with phytochemical analyses to isolate and determine the quantity of the most potent active ingredients.

Acknowledgements

Not applicable.

Funding

The present study was supported by Deanship of Academic Research at the University of Jordan (grant no. 19/2021/528).

Availability of data and materials

All data generated or analyzed during this study are included in this published article.

Authors' contributions

AI and AAZ conceived the study, designed and performed the experiments, analyzed data and wrote the manuscript. TAT designed and performed the experiments and wrote the manuscript. WAA designed the experiments and wrote the manuscript. HAA designed the experiments and analyzed data. MZ analyzed data. AA designed and performed the experiments, analyzed data and wrote the manuscript. AI and AA confirm the authenticity of all the raw data. All authors have read and approved the final manuscript.

Ethics approval and consent to participate

The experimental protocol was approved by the Animal Ethics Committee at the University of Jordan (approval no. 47-2022; Amman, Jordan).

Patient consent for publication

Not applicable.

Authors' information

Asma' Al-Zabin, orcid.org/0009-0008-4795-4019 Amer Imraish, orcid.org/0000-0003-1191-2905 Malik Zihlif, orcid.org/0000-0002-8005-3908 Tuqa Abu Thiab orcid.org/0000-0002-3054-4047 Wajdy Al-Awaida, orcid.org/0000-0003-3095-2224 Hamzeh J. Al-Ameer, orcid.

org/0000-0002-1681-6747 Afnan Al-Hunaiti, orcid.org/0000-0002-0740-1179.

Competing interests

The authors declare that they have no competing interests.

References

1. Rao MD and Gautam P: Synthesis and characterization of ZnO nanoflowers using Chlamydomonas reinhardtii: A green approach. Environmental Progress & Sustainable Energy 35: 1020-1026, 2016.
2. Khan S, Mansoor S, Rafi Z, Kumari B, Shoaib A, Saeed M, Alshehri S, Ghoneim MM, Rahamathulla M, Hani U and Shakeel F: A review on nanotechnology: Properties, applications, and mechanistic insights of cellular uptake mechanisms. J Mol Liquids 348: 118008, 2022.
3. Sogno I, Venè R, Ferrari N, De Censi A, Imperatori A, Noonan DM, Tosetti F and Albini A: Angioprevention with fenretinide: Targeting angiogenesis in prevention and therapeutic strategies. Crit Rev Oncol Hematol 75: 2-14, 2010.
4. Mohammad GRKS, Tabrizi MH, Ardalan T, Yadamani S and Safavi E: Green synthesis of zinc oxide nanoparticles and evaluation of anti-angiogenesis, anti-inflammatory and cytotoxicity properties. J Biosci 44: 30, 2019.
5. Adeola FO: Global impact of chemicals and toxic substances on human health and the environment. Handbook of Global Health, 2020: p. 1-30.
6. Vimalraj S, Ashokkumar T and Saravanan S: Biogenic gold nanoparticles synthesis mediated by Mangifera indica seed aqueous extracts exhibits antibacterial, anticancer and anti-angiogenic properties. Biomed Pharmacother 105: 440-448, 2018.
7. Imade EE, Ajiboye TO, Fadiji AE, Onwudiwe DC and Babalola OO: Green synthesis of zinc oxide nanoparticles using plantain peel extracts and the evaluation of their antibacterial activity. Sci African 16: e01152, 2022.
8. Mohammadian M, Es'haghi Z and Hooshmand S: Green and chemical synthesis of zinc oxide nanoparticles and size evaluation by UV-vis spectroscopy. J Nanomed Res 7: 00175, 2018.
9. Sukhanova A, Bozrova S, Sokolov P, Berestovoy M, Karaulov A and Nabiev I: Dependence of nanoparticle toxicity on their physical and chemical properties. Nanoscale Res Lett 13: 44, 2018.
10. Folkman J: Role of angiogenesis in tumor growth and metastasis. Semin Oncol 29 (6 Suppl 16): S15-S18, 2002.
11. Lacerda JZ, Ferreira LC, Lopes BC, Aristizábal-Pachón AF, Bajgelman MC, Borin TF and Zuccari DAPC: Therapeutic potential of melatonin in the regulation of MiR-148a-3p and angiogenic factors in breast cancer. Microrna 8: 237-247, 2019.
12. Melincovici CS, Boşca AB, Şuşman S, Mărginean M, Mihu C, Istrate M, Moldovan IM, Roman AL and Mihu CM: Vascular endothelial growth factor (VEGF)-key factor in normal and pathological angiogenesis. Rom J Morphol Embryol 59: 455-467, 2018.
13. Tahvilian R, Zangeneh MM, Falahi H, Sadrjavadi K, Jalalvand AR and Zangeneh A: Green synthesis and chemical characterization of copper nanoparticles using Allium saralicum leaves and assessment of their cytotoxicity, antioxidant, antimicrobial, and cutaneous wound healing properties. Applied Organometallic chemistry 33: e5234, 2019.
14. Shadmehri AA, Namvar F, Miri H, Yaghmaei P and Moghaddam MN: Anti-Angiogenesis effect of graphene-loaded green synthesized zinc oxide nanoparticles on chick chorioalantoic membrane. J Biotechem Tec 17-22, 2018.
15. Cui L, Liang J, Liu H, Zhang K and Li J: Nanomaterials for angiogenesis in skin tissue engineering. Tissue Eng Part B Rev 26: 203-216, 2020.
16. Ahtzaz S, Nasir M, Shahzadi L, Amir W, Anjum A, Iqbal F, Chaudhry AA, Yar M and ur Rehman I: A study on the effect of zinc oxide and zinc peroxide nanoparticles to enhance angiogenesis-pro-angiogenic grafts for tissue regeneration applications. Materials & Design 132: 409-418, 2017.
17. Newman DJ, Cragg GM and Snader KM: Natural products as sources of new drugs over the period 1981-2002. J Nat Prod 66: 1022-1037, 2003.
18. El-Shafey ES and Elsherbiny ES: The role of apoptosis and autophagy in the insulin-enhancing activity of oxovanadium (IV) bipyridine complex in streptozotocin-induced diabetic mice. Biometals 33: 123-135, 2020.
19. El Seedy GM, El-Shafey ES and Elsherbiny ES: Ziziphus spina-christi (L.) fortified with Camellia sinensis mediates apoptosis, Notch-1 signaling, and mitigates obesity-induced non-alcoholic fatty liver. J Food Biochem: Jul 9, 2021 (Epub ahead of print).
20. Sahan Y, Dundar AN, Aydin E, Kilci A, Dulger D, Kaplan FB, Gocmen D and Celik G: Characteristics of cookies supplemented with oleaster (Elaeagnus angustifolia L.) Flour. I physicochemical, sensorial and textural properties. Journal of Agricultural Science, 2013. 5: 160, 2013.
21. Ogunyemi SO, Abdallah Y, Zhang M, Fouad H, Hong X, Ibrahim E, Masum MMI, Hossain A, Mo J and Li B: Green synthesis of zinc oxide nanoparticles using different plant extracts and their antibacterial activity against Xanthomonas oryzae pv. oryzae. Artif Cells Nanomed Biotechnol 47: 341-352, 2019.
22. Choi HS, Ashitate Y, Lee JH, Kim SH, Matsui A, Insin N, Bawendi MG, Semmler-Behnke M, Frangioni JV and Tsuda A: Rapid translocation of nanoparticles from the lung airspaces to the body. Nat Biotechnol 28: 1300-1303, 2010.
23. Gürbüz I, Ustün O, Yesilada E, Sezik E and Kutsal O: Anti-ulcerogenic activity of some plants used as folk remedy in Turkey. J Ethnopharmacol 88: 93-97, 2003.
24. Chakraborty AJ, Mitra S, Tallei TE, Tareq AM, Nainu F, Cicia D, Dhama K, Emran TB, Simal-Gandara J and Capasso R: Bromelain a potential bioactive compound: A comprehensive overview from a pharmacological perspective. Life (Basel) 11: 317, 2021.
25. Yanez M, Blanchette J and Jabbarzadeh E: Modulation of inflammatory response to implanted biomaterials using natural compounds. Curr Pharm Des 23: 6347-6357, 2017.
26. Wang Y, Guo T, Li JY, Zhou SZ, Zhao P and Fan MT: Four flavonoid glycosides from the pulps of Elaeagnus angustifolia and their antioxidant activities. Adv Mater Res 756-759: 16-20, 2013.
27. Ahmadiani A, Hosseiny J, Semnanian S, Javan M, Saeedi F, Kamalinejad M and Saremi S: Antinociceptive and anti-inflammatory effects of Elaeagnus angustifolia fruit extract. J Ethnopharmacol 72: 287-292, 2000.
28. Mohammed FI, Al-Essa MK, Shafagoj YA and Afifi FU: Investigation of the direct effects of the alcoholic extract of Elaeagnus angustifolia L.(Elaeagnaceae) on dispersed intestinal smooth muscle cells of guinea pig. Sci Pharm 74: 21-30, 2006.
29. Imraish A, Abu Thiab T, Al-Awaida W, Al-Ameer HJ, Bustanji Y, Hammad H, Alsharif M and Al-Hunaiti A: In vitro anti-inflammatory and antioxidant activities of $ZnFe_2O_4$ and $CrFe_2O_4$ nanoparticles synthesized using Boswellia carteri resin. J Food Biochem 45: e13730, 2021.
30. Scherbakov AM, Vorontsova SK, Khamidullina AI, Mrdjanovic J, Andreeva OE, Bogdanov FB, Salnikova DI, Jurisic V, Zavarzin IV and Shirinian VZ: Novel pentacyclic derivatives and benzylidenes of the progesterone series cause anti-estrogenic and antiproliferative effects and induce apoptosis in breast cancer cells. Invest New Drugs 41: 142-152, 2023.
31. Jurisic V: Multiomic analysis of cytokines in immuno-oncology. Expert Rev Proteomics 17: 663-674, 2020.
32. Sanaeimehr Z, Javadi I and Namvar F: Antiangiogenic and antiapoptotic effects of green-synthesized zinc oxide nanoparticles using Sargassum muticum algae extraction. Cancer Nanotechnol 9: 3, 2018.
33. Abdalla AME, Xiao L, Ullah MW, Yu M, Ouyang C and Yang G: Current challenges of cancer anti-angiogenic therapy and the promise of nanotherapeutics. Theranostics 8: 533-548, 2018.
34. Kumar B, Smita K, Cumbal L and Debut A: Green approach for fabrication and applications of zinc oxide nanoparticles. Bioinorg Chem Appl 2014: 523869, 2014.
35. Tada-Oikawa S, Ichihara G, Suzuki Y, Izuoka K, Wu W, Yamada Y, Mishima T and Ichihara S: Zn (II) released from zinc oxide nano/micro particles suppresses vasculogenesis in human endothelial colony-forming cells. Toxicol Rep 2: 692-701, 2015.